Video Article

Use of Enzymatic Biosensors to Quantify Endogenous ATP or H_2O_2 in the Kidney

Oleg Palygin[1], Vladislav Levchenko[1], Louise C. Evans[1], Gregory Blass[1], Allen W. Cowley Jr.[1], Alexander Staruschenko[1]

[1]Department of Physiology, Medical College of Wisconsin

Correspondence to: Alexander Staruschenko at staruschenko@mcw.edu

URL: https://www.jove.com/video/53059
DOI: doi:10.3791/53059

Keywords: Molecular Biology, Issue 104, Biosensor, kidney, ATP, H_2O_2, rat, amperometry, purinergic signaling

Date Published: 10/12/2015

Citation: Palygin, O., Levchenko, V., Evans, L.C., Blass, G., Cowley Jr., A.W., Staruschenko, A. Use of Enzymatic Biosensors to Quantify Endogenous ATP or H_2O_2 in the Kidney. *J. Vis. Exp.* (104), e53059, doi:10.3791/53059 (2015).

Abstract

Enzymatic microelectrode biosensors have been widely used to measure extracellular signaling in real-time. Most of their use has been limited to brain slices and neuronal cell cultures. Recently, this technology has been applied to the whole organs. Advances in sensor design have made possible the measuring of cell signaling in blood-perfused *in vivo* kidneys. The present protocols list the steps needed to measure ATP and H_2O_2 signaling in the rat kidney interstitium. Two separate sensor designs are used for the *ex vivo* and *in vivo* protocols. Both types of sensor are coated with a thin enzymatic biolayer on top of a permselectivity layer to give fast responding, sensitive and selective biosensors. The permselectivity layer protects the signal from the interferents in biological tissue, and the enzymatic layer utilizes the sequential catalytic reaction of glycerol kinase and glycerol-3-phosphate oxidase in the presence of ATP to produce H_2O_2. The set of sensors used for the *ex vivo* studies further detected analyte by oxidation of H_2O_2 on a platinum/iridium (Pt-Ir) wire electrode. The sensors for the *in vivo* studies are instead based on the reduction of H_2O_2 on a mediator coated gold electrode designed for blood-perfused tissue. Final concentration changes are detected by real-time amperometry followed by calibration to known concentrations of analyte. Additionally, the specificity of the amperometric signal can be confirmed by the addition of enzymes such as catalase and apyrase that break down H_2O_2 and ATP correspondingly. These sensors also rely heavily on accurate calibrations before and after each experiment. The following two protocols establish the study of real-time detection of ATP and H_2O_2 in kidney tissues, and can be further modified to extend the described method for use in other biological preparations or whole organs.

Video Link

The video component of this article can be found at https://www.jove.com/video/53059/

Introduction

Enzymatic microelectrode biosensors (also referenced as sensors in the present manuscript) have been a valuable tool for studying dynamic signaling processes in living cells and tissues. The sensors provide increased temporal and spatial resolution of cell signaling molecules in biologically relevant concentrations. Instead of sampling and analyzing extracellular fluids taken at intervals over long periods of time, these sensors respond as fast as their enzymes react to the analyte, thereby producing real-time measurements[1,2]. Fast detection of interstitial concentrations of autocrine and paracrine factors, like purines or hydrogen peroxide, and the dynamics of their release can be used to establish a profile for the effects of drugs in normal and pathological conditions [3]. Currently, the majority of applications using sensors have been in brain tissue slices and cell cultures[4-10]. The protocols detailed in this manuscript aim to establish the means to accurately measure real-time concentrations of analytes in whole kidneys.

The following protocols were developed to study interstitial ATP and H_2O_2 signaling in kidneys. In the native environment of the kidney, extracellular ATP is rapidly catabolized by endogenous ectonucleotidases into its derivatives (ADP, AMP and adenosine). The sensors used here are highly selective to ATP over other purines or ATP degradation products[11]. This offers a great advantage as it allows accurate monitoring of the constant and dynamic concentrations of ATP release and its signaling function. Interstitial ATP concentration is measured using the combination of two microelectrodes, an ATP sensor and a Null sensor. The Null sensor in combination with catalase applications is able to detect interstitial H_2O_2 concentrations[12]. The following protocols use two different designs of sensors that have characteristics optimal for either *ex vivo* or *in vivo* applications.

Both designs are based on the sequential catalytic reaction of glycerol kinase and glycerol-3-phosphate oxidase contained in a sensor enzymatic layer and is driven by the presence of ATP. In the set of sensors used in the *ex vivo* studies, H_2O_2, the final enzymatic reaction product, is detected by oxidation on a platinum/iridium (Pt-Ir) wire electrode. Sensors for *in vivo* studies are instead based on H_2O_2 reduction on a mediator coated gold electrode designed for blood-perfused tissue. Shown in **Figure 1** is a scheme of both protocols described in this manuscript. The Null sensor is identical to its corresponding ATP sensor except it lacks the bound enzymes. Therefore, in addition to the detection of H_2O_2 with the catalase enzyme, the Null sensor measures nonspecific interferences. ATP concentrations are calculated by subtracting the Null detected nonspecific interferences and background H_2O_2 from the ATP sensor signal. Several sensors are also commercially available to detect other

analytes including adenosine, ionosine, hypoxanthine, acetylcholine, choline, glutamate, glucose, lactate, d-serine for *ex vivo* applications or adenosine, ionosine, and hypoxanthine for *in vivo* when paired with the corresponding Null sensor.

The ability of the sensor to accurately detect analytes depends on the proper pre- and post- calibrations[13]. This ensures that the analysis accounts for the drift in sensor sensitivity that occurs during use in biological tissues. The sensor holds a depot of glycerol that is used as a reagent in the sensor enzymatic reactions. If the sensor is not used in bath solutions containing glycerol, it will wash out over time. Shorter recording times are then necessary to minimize the sensor drift. Additionally sensor fouling by endogenous proteases and protein fragments can greatly diminish the sensitivity of the sensors[14].

The present manuscript establishes the use of enzymatic microelectrode biosensors for *ex vivo* and *in vivo* kidney preparations. Real-time analyte quantification provides unprecedented detail of cellular signaling that may reveal novel insights into the mechanisms of kidney diseases and pharmacological agents.

Protocol

The following animal procedures adhered to the NIH Guide for the Care and Use of Laboratory Animals. Prior approval was obtained from the Institutional Animal Care and Use Committee (IACUC).
NOTE: Review of the sensor manufacturer instructions should be done during the experiment design and prior to their use. Following these instructions will produce optimal results when using the sensors.

1. Sensor Calibration

1. Prepare fresh stock solutions prior the start of the experiment.
2. Create Buffer A containing 10 mM NaPi buffer, 100 mM NaCl, 1 mM $MgCl_2$, and 2 mM glycerol. Adjust the pH to 7.4 using NaOH. Store at 2-8 °C.
3. Using a stock ATP concentration (100 mM) stored at -20 °C, create a fresh 10 mM ATP calibration solution by adding 10 µl stock to 90 µl of Buffer A.
4. Rehydrate the ATP sensor by placing its tip (**Figure 2**) into the rehydration chamber containing Buffer A for at least 10 min at 2-8 °C.
   NOTE: After rehydration, the sensors should not be exposed to air for more than 20 sec or the sensor sensitivity may be reduced. If long exposures to air are anticipated, dip the sensor briefly into a solution of glycerol. The sensors may be used for multiple experiments but these must occur on the same day as sensor rehydration. The sensors can be stored in the rehydration chamber with Buffer A for up to 24 hr.
5. Turn on the dual channel potentiostat (**Figure 3**) and start the recording system software.
6. Prepare a calibration chamber with 3 ml of Buffer A. Place the reference electrode into the calibration chamber. Take each sensor from the rehydration chamber, then attach it to the manipulator and insert it into the calibration chamber solution.
   NOTE: Use a standard silicone coated petri dish as a calibration chamber. Carry out all calibrations and studies in a Faraday cage on a high-performance lab air table to reduce signal noise during the amperometry recordings (**Figure 4**). Calibrations are best done as close to the start of data collection as possible. For *in vivo* applications the optimal time for calibration is during the animal post-surgery recovery period.
7. *Ex vivo* calibration
   1. Perform cyclic voltammetry in the calibration chamber by cycling the sensors from -500 mV to +500 mV at a rate of 100 mV/sec for 10 cycles. This greatly improves the sensitivity of the sensors. See **Figure 5** for the traces observed from the 10 cycles.
   2. Polarize the sensors to +600 mV after the last cycle. The sensor current will decay to an asymptote. A steady reading is achieved after a minimum of 5 min. Record the zero reading.
8. *In vivo* sensor calibration
   1. Do not perform the cyclic voltammetry on the *in vivo* sensors. Instead, polarize the sensor in the calibration chamber for 30 sec to +500 mV. Then set the potentiostat to 0 mV and allow the sensor current to rise to an asymptote. The sensor current will take at least 2 min to asymptote. Record the zero reading.
9. Consecutively add set amounts of ATP solution into the chamber to produce a calibration line encompassing a desired detection range. The ATP solution produces a sharp peak in the sensor signal initially, followed by a decay as the ATP diffuses evenly throughout the chamber. Record signal values once the signal level has stabilized after each ATP addition. **Figures 6A and 7** show traces and suggested ATP concentrations for both *ex vivo* and *in vivo* studies, respectively.
   NOTE: It is important to confirm the selectivity of the electrodes by using scavengers of the analytes. The present protocol used apyrase to test the specificity of the ATP sensor and catalase for the H_2O_2 signal (**Figures 6B**). If drugs are to be administered, measurements of their reactivity with the sensors should be determined before the study.
10. Add 3 µl of apyrase from a stock of 2 mg/ml (89 UN/mg) to test specificity of the ATP sensor (the current produced by ATP application should reduce to the zero level (**Figure 7**).
11. Add 3 µl of catalase from a stock of 2mg/ml (100 UN/mg) to test the specificity of the null sensor (the current produced by H_2O_2 application should reduce to the zero reading).

2. Animal Surgery For Sensor Studies

1. Surgery for *ex vivo*
   1. Anesthetize the experimental animal with isoflurane (5% induction, 1.5 to 2.5% maintenance)/medical grade O_2 or another approved method. [15, 12] Animals must be continually monitored to ensure an adequate level of anesthesia. Stable respiratory rate and toe pinch reaction are used to confirm proper anesthesia.
      Note: Euthanize the animal according to approved IACUC protocols. At the completion of all non-survival procedures euthanize deeply anaesthetized animals by thoracotomy inducing pneumothorax to ensure the humane demise of the animal[12].

2. Place the rat on a temperature-controlled surgical table in a supine position. While maintaining a proper anesthetic depth, make a midline incision of approximately 5 cm in line with the left kidney and expose the distal abdominal aorta.
3. Wrap a ligature around the celiac and superior mesenteric arteries, and the abdominal aorta above these arteries but do not ligate. Wrap two ligatures around the abdominal aorta below the renal arteries.
4. Clamp the abdominal aorta above the ligatures. Tie the lower ligature. Catheterize the abdominal aorta with polyethylene tubing (PE50). Secure the catheter with the second aorta ligature.
5. Remove the clamp and ligate the mesenteric and celiac arteries. Perfuse the kidney at 6 ml/min with Hanks Balanced Salt Solution at RT for 2-3 min until the kidney is completely blanched.
6. Excise the kidney and the catheter, connected portion of the aorta. Place the kidney into a 3 ml Petri dish filled with bath solution.
Note: Experiment protocol can be performed at RT. The bath solution contains in mM: 145 NaCl, 4.5 KCl, 2 $MgCl_2$, 1 $CaCl_2$, 10 HEPES, pH 7.35 adjusted with NaOH.

2. Surgery for *in vivo*
1. Anesthetize the rat using approved IACUC protocols. For *in vivo* analysis anesthetize the rats with ketamine (20 mg/kg *i.m.*) and inactin (50 mg/kg *i.p.*). Animals must be continually monitored to ensure an adequate level of anesthesia. A stable respiratory rate and toe pinch reaction are used to confirm proper anesthesia.
2. After proper anesthesia depth is obtained, place the rat in a supine position on a temperature-controlled grounded surface located on the air table. The surface should be preheated and maintained at 36 °C.
3. While maintaining proper anesthetic depth, make a midline incision approximately 5 cm in line with the kidney.
4. Use a suture to deflect and anchor the cutaneous and subcutaneous tissue so that the entire kidney is visible. Place the kidney in a kidney cup to minimize any movement artifacts.
5. Use an IV infusion of 2% BSA: 0.9% NaCl at 1 ml/100 g/hr via the jugular vein to maintain blood volume. Cannulate both ureters for urine collection. Place ties around the superior mesenteric and celiac arteries and the distal aortal for the manipulation of renal perfusion pressure (**Figures 10A**).
6. If the application of pharmacological agents is required during the *in vivo* experiments, insertion of an interstitial catheter is recommended (**Figures 10B**).

3. Data Acquisition Setup

1. Open the data acquisition program and set its polarity for both *ex vivo* and *in vivo* experiments to Anodic Positive. Set the program to save data as ASCII code.
2. Position the micromanipulators for quick insertion of the sensors into the kidneys.
NOTE: Alternatively, use a dummy probe attached to the micromanipulator to help achieve the desired placement of sensors.
3. *Ex vivo* data acquisition
1. Perfuse the kidney with bath solution (from 2.1.6) via the cannulated aorta at a constant rate of 650 µl/min. Using surgical scissors, carefully remove the kidney capsule, which is necessary for sensor insertion.
2. Secure the kidney with rubber bands strapped over the kidney and attached to the silicone-coated dish with pins.
3. Place the reference electrode close to the kidney in the petri dish with its tip submerged in the buffer solution.

4. *In vivo* data acquisition
1. Place the kidney in a kidney cup. Depending on the strain and age of the animal use a size of cup that holds the kidney loosely. **Figure 8** shows two sizes of kidney cups. Similar cups are used for different physiological approaches focused on the analysis of kidney function such as micropuncture etc[16].
Note: The position of the kidney cup is critical to remove the mechanical noise produced by the animal breathing but should not interfere with or block kidney perfusion or urine flow.
2. Allow 45 min of recovery time before performing data collection.
3. Using a 26-30G needle, make a puncture hole at the desired location and depth of the sensor in the kidney. Blot the surface hole to remove exuded blood. Add glycerol solution to the surface of the kidney. This will prevent the kidney surface from drying out during the experiment.
4. Remove the first sensor from the rehydration chamber and attach it to the micromanipulator. Quickly, within 20 sec, insert the electrode into the freshly created hole in the kidney. Repeat steps 3.5-3.9 for the null sensor.
5. Insert the reference electrode into the kidney, approximately 1 cm from from the sensors.

5. Turn on the potentiostat and activate the recording program on the computer. **Figure 9** shows the final setup of the *ex vivo* kidney data acquisition. **Figure 10** shows the final setup of the *in vivo* kidney data acquisition with an inserted catheter.

4. Data Analysis

1. Import the ASCII data file into Origin or any other similar software.
2. Concentration current relation
1. Use the linear fit/extrapolate function to build a linear concentration (*x*-axis) to current (*y*-axis) relationship for the ATP or H_2O_2 calibration points (**Figures 6 and 7**).
linear fit line: y = mx + b

3. Equate the current to concentration
4. Subtract the measured traces of the null sensor from those of the ATP sensor to obtain the actual current produced by intracellular ATP.

5. Convert the ATP values in pA obtained by amperometry to nM using the calibration equation detailed in 4.2.1. Determine the concentration of the subtracted data trace of the ATP sensor by importing each adjusted current into the "x" value and solving for y (the concentration of analyte).
6. Similarly, calculate H_2O_2 concentration from its calibration equation if needed.

Representative Results

The design of the enzymatic microelectrode biosensor allows the real-time detection of analytes in whole kidneys. The general experiment design for either *ex vivo* or *in vivo* studies is illustrated in **Figure 1**.The sensors used and the surgical procedures differ depending on whether the study is *ex vivo* or *in vivo*.

To obtain reproducible results, accurate pre- and post- calibrations are critical. **Figure 6A** shows a representative trace of the signal seen from the *ex vivo* ATP sensor during calibrations. Note that apyrase quickly eliminated the ATP signal. Catalase had no effect on the ATP signal and demonstrates its specificity to the H_2O_2 it creates (**Figure 6B**). The calibration procedure produces a linear fit that is used to calculate the dynamic changes of ATP (**Figure 6A, right panel**). *In vivo* sensor calibration produces a similar trace to that of the *ex vivo* sensor. However, this sensor detects reductive instead of oxidative currents and as such the current produced is negative. Calibration of these sensors also produces a linear fit in a 0.3 to 80 µM range (**Figure 7A right panel**). Specificity of *in vivo* sensor to ATP over other purine products is shown in **Figure 7B**.

The approach described here allows us to measure both basal levels of endogenous substances and acute changes in response to drug infusion[12]. Shown in **Figure 11** are Ang II-induced changes of interstitial endogenous concentration of H_2O_2 in salt-resistant and salt-sensitive rats. For these experiments, freshly isolated kidneys from Sprague Dawley (SD) or Dahl salt-sensitive (SS) rats were perfused with 1 µM Ang II under constant laminar flow (650 µl/min). As shown in **Figure 11**, Ang II induces the acute release of H_2O_2 in kidneys from both SD and SS rats. However, the maximum amplitude of each response was significantly elevated in SS rats, especially when the animals were fed with a high salt diet[12]. Shown in **Figure 12** is a representative application of the biosensors *in vivo*. The infusion of catalase (5 µg/ml) completely blocks the H_2O_2 signal detected by the biosensor. These experiments illustrate the use of specific enzymatic biosensors combined with the amperometric technique for the detection of basal levels of endogenous substances and real-time measurements of their release in response to pharmacological intervention. Further applications of this approach to study the role of purinergic signaling and hydrogen peroxide will improve our knowledge and understanding of renal pathologies like salt-sensitive hypertension, renal oxidative stress and chronic kidney disease.

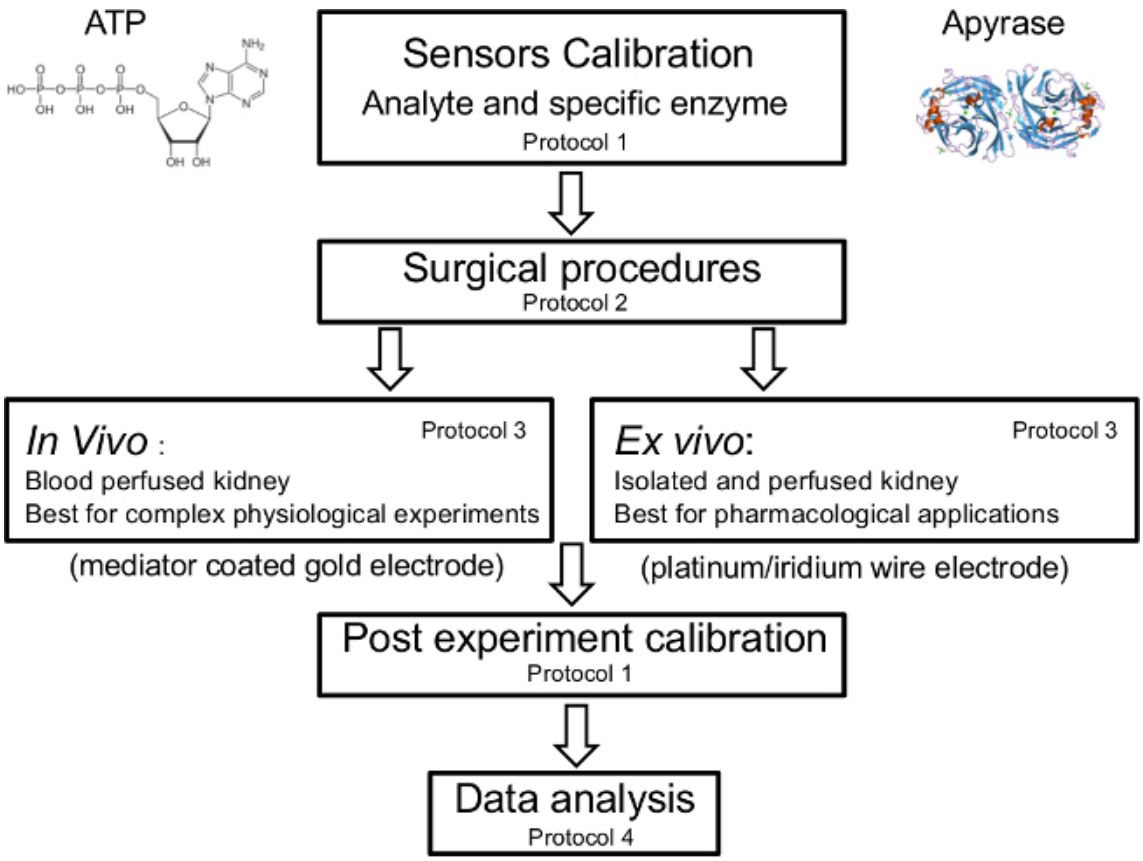

Figure 1. Schematic of the Protocols. Calibration with analyte of interest and testing its specificity is done immediately prior to the start of the experiments. The *in vivo* protocol should be followed for complex physiological experiments and *ex vivo* for pharmacological applications. Post experiment calibration should be done and taken into account during the data analysis. Please click here to view a larger version of this figure.

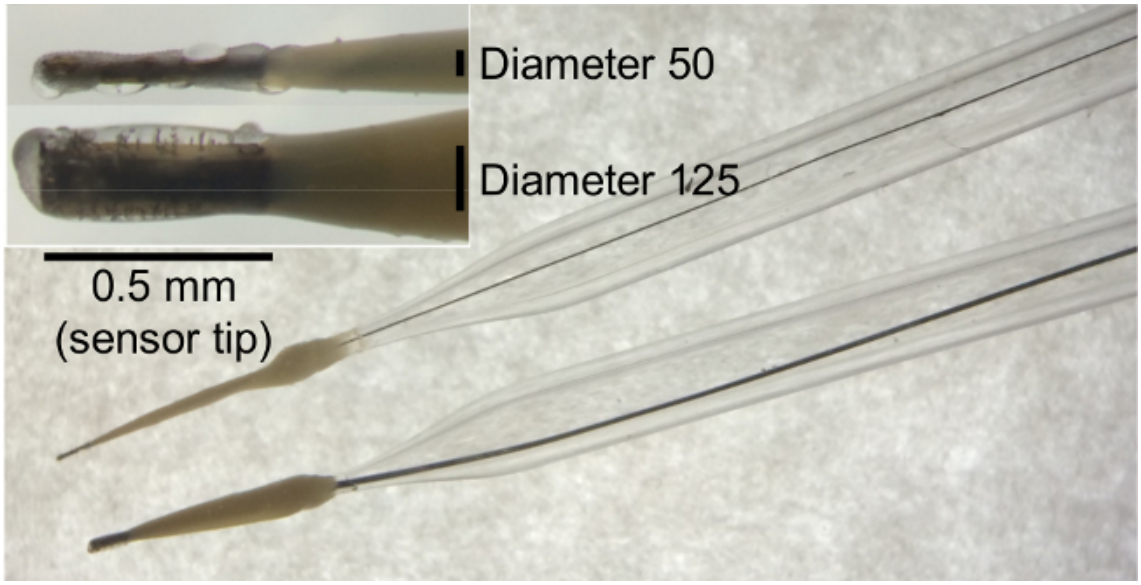

Figure 2. Enzymatic Microelectrode Sensor. The two sensor sizes used for *ex vivo* applications are shown, 50 µm and 125 µm diameters. Each sensor wire extends into a capillary tube to connect to a gold end connector (not shown). Inset shows a sensor tip coated with enzymes for ATP detection. Please click here to view a larger version of this figure.

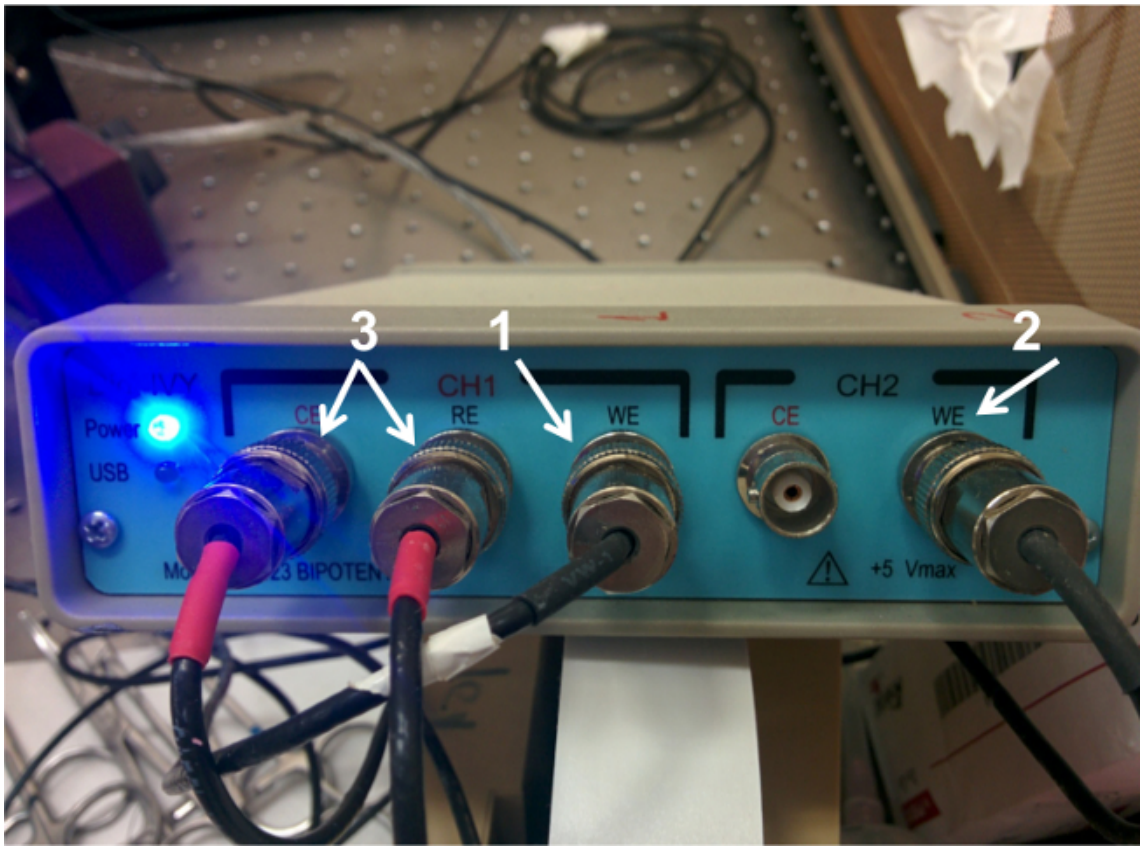

Figure 3. Dual Channel Potentiostat. The potentiostat channels labeled CH1 and CH2. 1) CH1 the ATP sensor connection and 2) CH2 the Null sensor connection 3) connections that are electrically coupled to the reference electrode. Please click here to view a larger version of this figure.

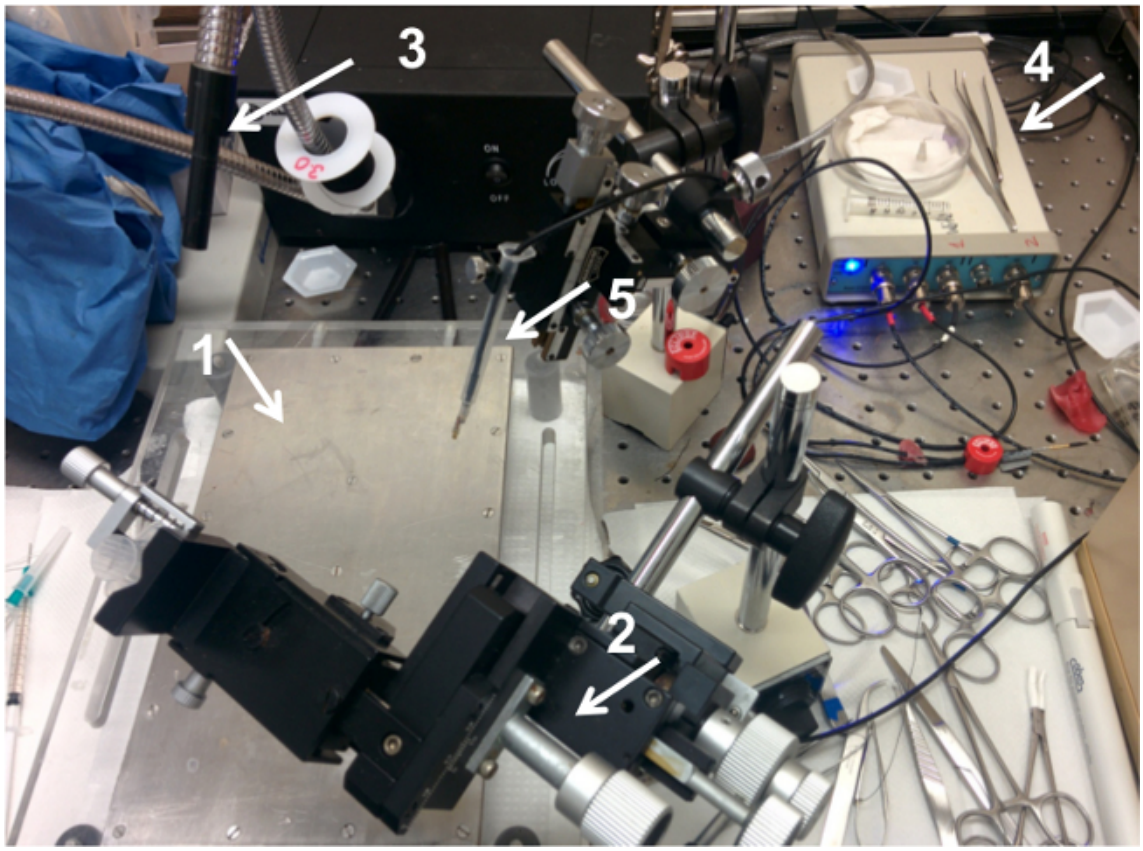

Figure 4. Sensor Setup. The data acquisition is performed in a Faraday cage to reduce electrical noise and on a high-performance lab table for a vibration-free working surface. 1) A temperature-controlled surgical table is used to maintain animal body temperature during physiological experiments 2) the micromanipulators are attached to magnetic mounting adaptors for flexible positioning of the sensors during experiment 3) A light source is needed for surgical procedures and sensor insertion 4) dual channel potentiostat 5) holder for the sensors. Please click here to view a larger version of this figure.

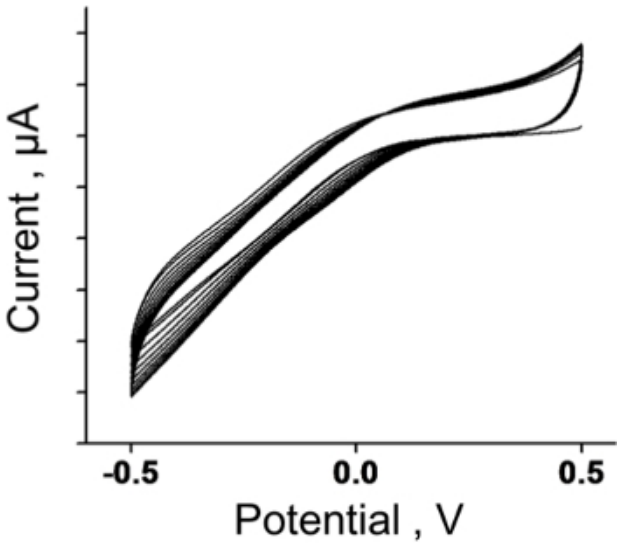

Figure 5. Cyclic Voltammetry. For *ex vivo* studies, sensor cyclic voltammetry is conducted for 10 cycles between -0.5 and 0.5 V prior to the calibration protocol. Please click here to view a larger version of this figure.

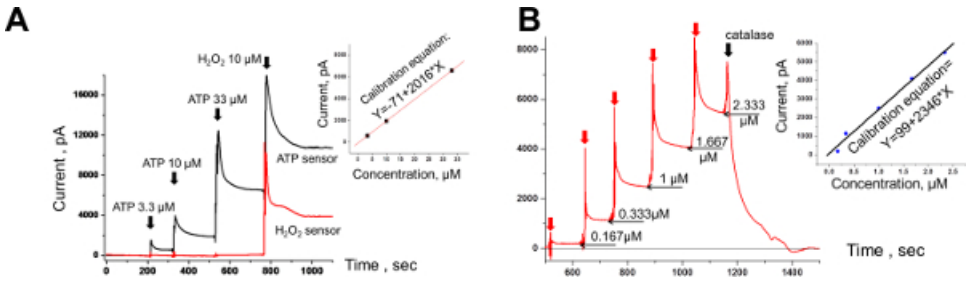

Figure 6. Amperometry Calibration for *Ex Vivo*. (**A**) Calibration uses the addition of known ATP concentrations to the bath solution. Corresponding amperometric values recorded at the asymptote level (black trace). The currents obtained create a calibration equation. An example is shown on the right panel. The red trace is the current of the Null sensor which responds to only the addition of H_2O_2. (**B**) The Null sensor is calibrated with the addition of known H_2O_2 concentrations (red arrows) to the bath solution and the asymptotes amperometric values are recorded (thin black arrows). Addition of catalase to the bath solution (thick black arrow) results in rapid current decay. The right panel shows the Null sensor calibration equation. Please click here to view a larger version of this figure. Please click here to view a larger version of this figure.

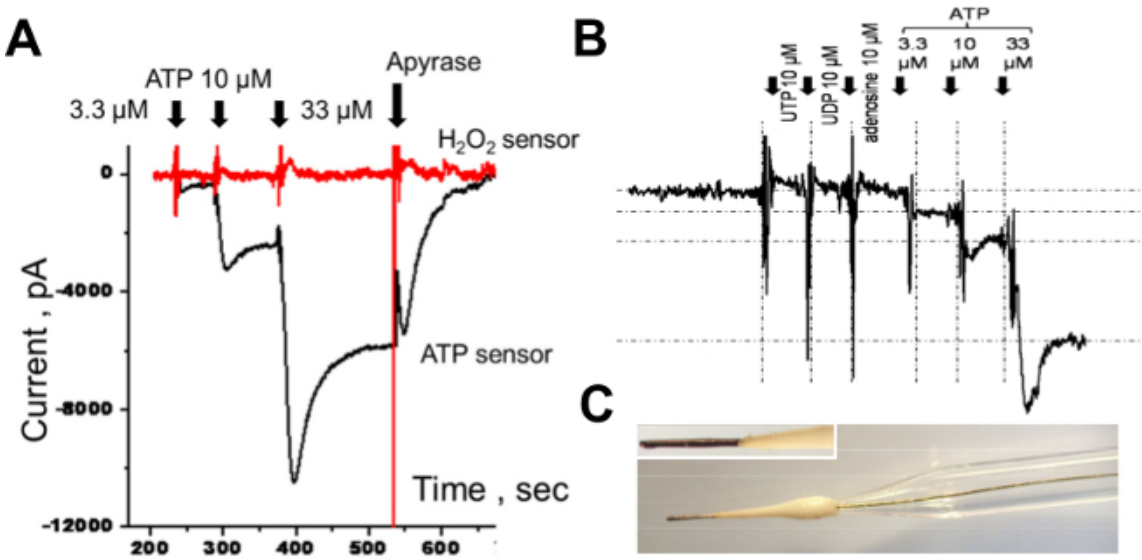

Figure 7. Amperometry Calibration for *In Vivo*. Calibration of the *in vivo* electrodes is performed in a similar fashion to that detailed in the *ex vivo* studies except reduction reactions cause a reverse current (polarity). (**A**) The addition of known ATP concentrations produces an amperometric current on the ATP sensor (black trace) but has no effect on the Null sensor (red trace). Addition of apyrase extinguishes the current of the ATP sensor. (**B**) The specificity of the ATP sensor is confirmed by the addition of 10 µM of different purinergic agents (UTP, UDP and adenosine). Further applications of ATP provide a stable detectable amperometric current. (**C**) Microphotograph of the *in vivo* sensors based on a mediator coated gold electrode. Please click here to view a larger version of this figure.

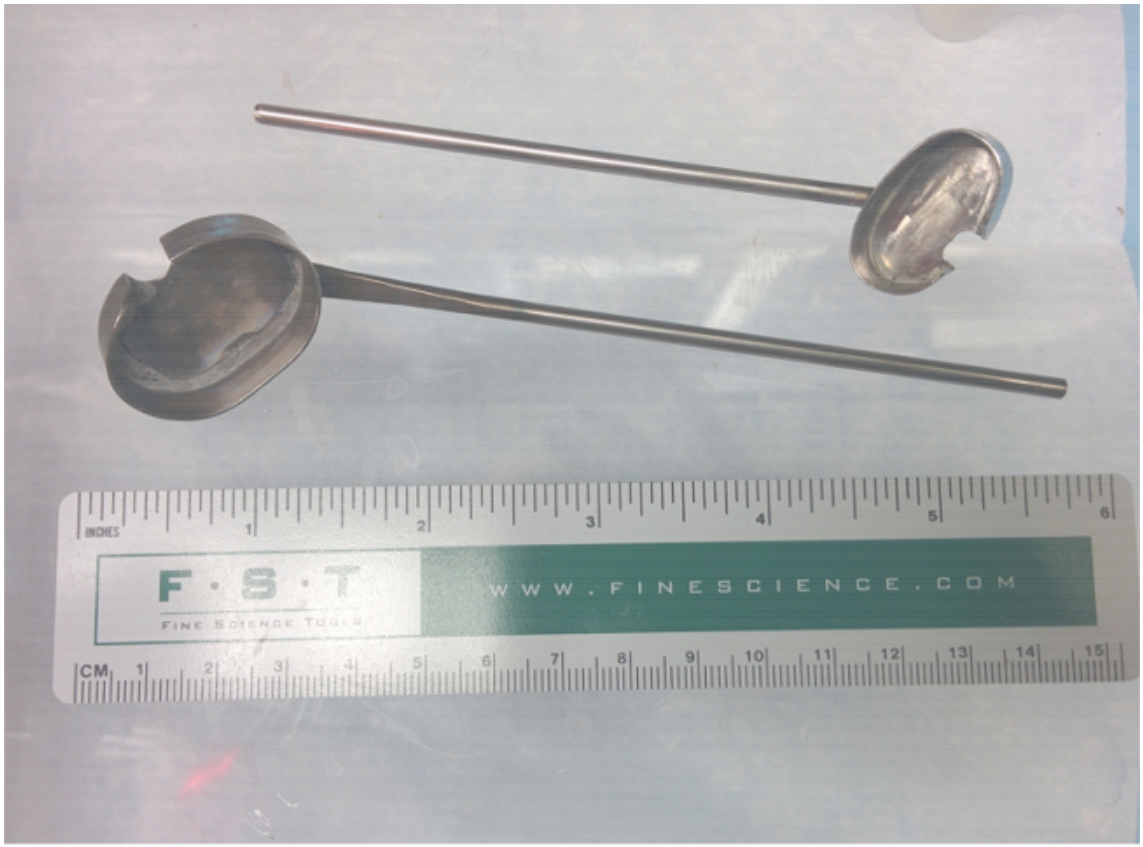

Figure 8. Kidney Cups. In the *in vivo* studies, kidneys are held still using the stainless steel kidney cups shown. Two sizes of cups are used to accommodate kidney size variation. These cups reduce the movement artifacts which are generated by the animal's respiration. Please click here to view a larger version of this figure.

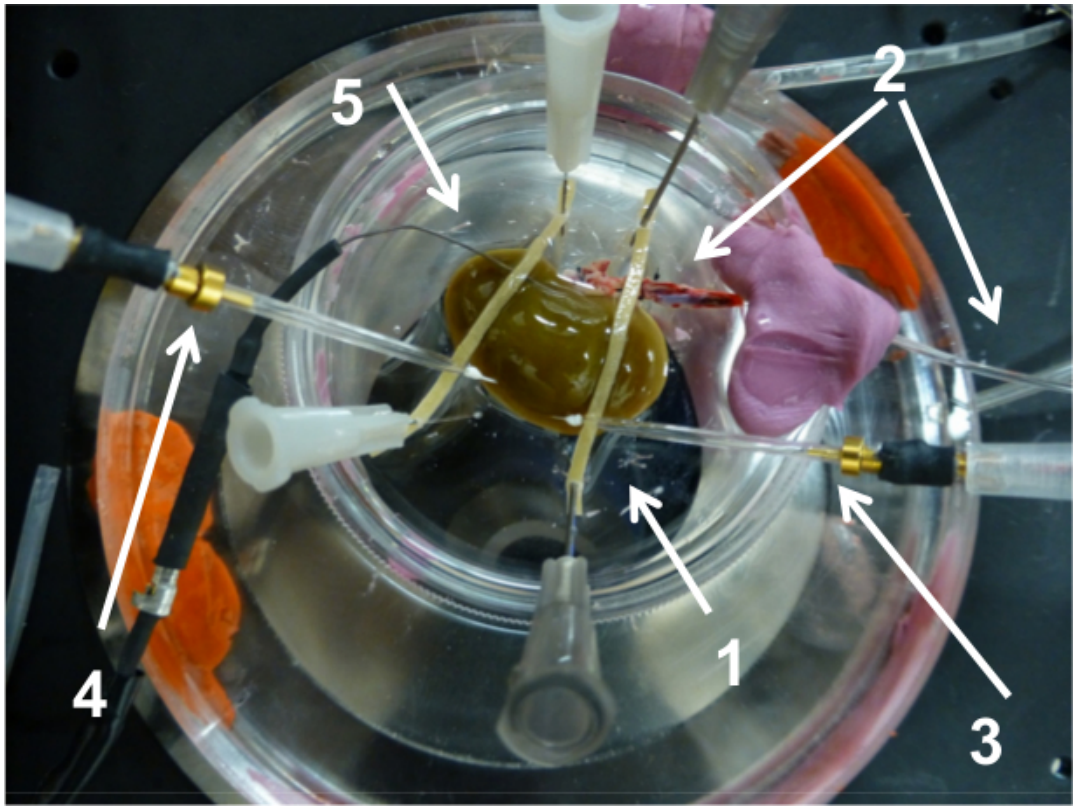

Figure 9. *Ex Vivo* Isolated and Perfused Kidney. The isolated kidney is placed into a 1) Petri dish coated with a thick silicone bottom for pin insertion 2) the renal artery is cannulated and attached to a syringe pump for constant perfusion during experiment 3) the ATP sensor, 4) and Null sensor are inserted into the kidney 5) the reference electrode is placed near the kidney submerged into the bath solution. Please click here to view a larger version of this figure.

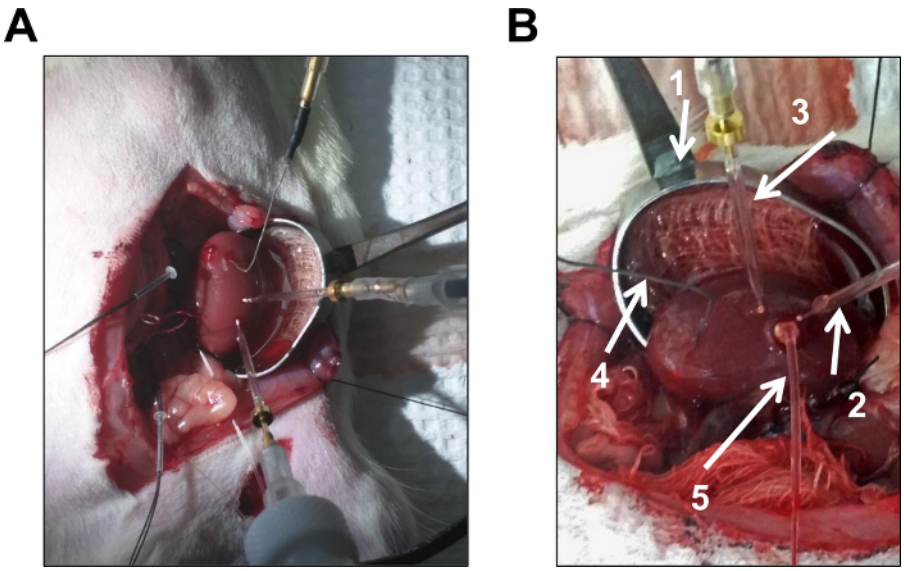

Figure 10. *In Vivo* Blood Perfused Kidney. (**A**) The left kidney is exposed and placed in a kidney cup, the right kidney remains intact inside the animal. Both sensors are inserted into the kidney. BSA:NaCl is infused via the catheterized jugular vein to counteract the fluid loss caused by the large mid-line incision (**B**) Example of the *in vivo* experiment with an implanted interstitial catheter for direct pharmacological applications 1) the kidney is held by a kidney cup 2) ATP sensor 3) Null sensor and 4) reference electrode are inserted into the ventral surface of the kidney 5) catheter implanted into the kidney and attached to a peristaltic pump for laminar pharmacological infusions. Please click here to view a larger version of this figure. Please click here to view a larger version of this figure.

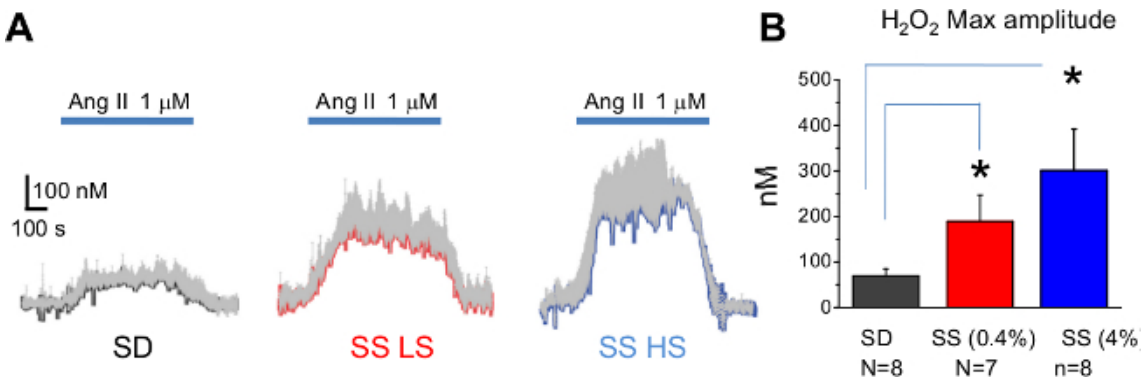

Figure 11. *Ex Vivo* Analysis of H_2O_2 in the kidney. Ang II perfusion causes H_2O_2 release in the rat kidney cortex. (**A**) Real time changes of the mean H_2O_2 concentration (gray bars show standard error) from a total of N = 8 applications (4 kidneys from 4 different rats). Bars on the top represent Ang II application. (**B**) The maximal H_2O_2 concentration amplitude values during Ang II perfusion for Sprague Dawley (SD) and Dahl salt-sensitive (SS) rats fed a low and high salt diets, respectively. * - $P < 0.05$ versus SD rats. The figure is adapted from reference[12] with permission. Please click here to view a larger version of this figure.

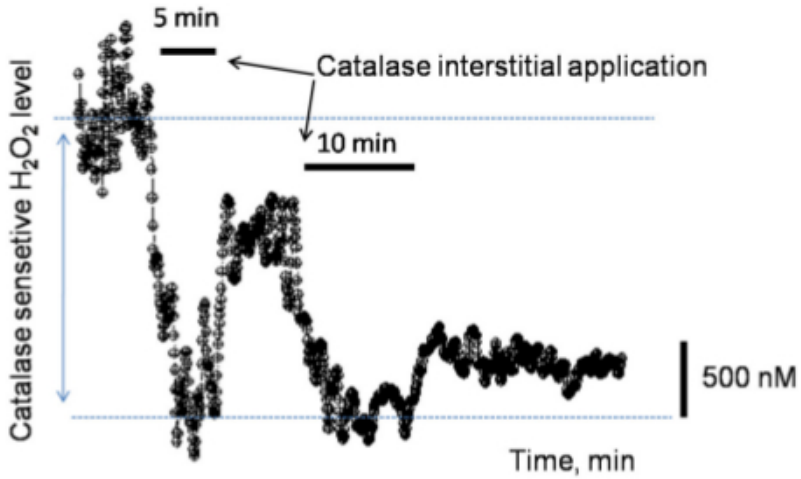

Figure 12. *In Vivo* Analysis of H_2O_2. Example of the *in vivo* assessment of interstitial H_2O_2 concentration in the medulla of a SS rat fed a low salt diet (as shown in **Figure 10B**). The interstitial application of catalase via an implanted catheter for the 5 min interval produced a complete blockade of the H_2O_2 signal in the renal medulla. Reduction of catalase, from washout by renal blood flow, resulted in a partial recovery of the signal, which was blocked again by an additional catalase application (10 min). Please click here to view a larger version of this figure.

Discussion

The present protocols were developed to provide enhanced temporal and spatial resolution of ATP and H_2O_2 signaling for *ex vivo* isolated, perfused and *in vivo* blood-perfused kidneys. The differences between the protocols and the sensors used here provide optimal data acquisition for either pharmacological agents or physiological studies. The protocols consist of 1) sensor calibration, 2) surgical procedure, 3) data acquisition setup, and 4) data analysis. They enable the real-time measurements of analytes for numerous experimental conditions. This will lead to greater insights into kidney diseases and the development of more effective pharmacological treatments. Here we used the sensors to analyze ATP and H_2O_2. However, sensors for other substances are also available and can be used. The protocols described here were applied to study ATP and H_2O_2 in rat kidneys, but the same method can easily be adjusted for application in mice. Thus, this approach has a great potential considering the abundance of genetic rodent models.

The basic design of enzymatic microelectrode biosensors was developed in the 1960's by Clark and Lyons[2]. Following the initial development of biosensors, advances have been made in both design[17-19] and applications[20]. Llaudet *et al.*[21,22] developed the principle design of the ATP sensors used in the present protocols while using methods from Cosneir *et al.*[23] for the enzyme coating. These sensors have detected ATP signaling in a number of physiological processes including ATP release from brain astrocytes[8], regulation of breathing[4,24], and skeletal muscle arteriole regulation[25]. Recently the *ex vivo* protocol has been used to measure ATP signaling in kidneys[12]. The goal of this manuscript is to provide effective directions and insights for the detection of endogenous substances such as ATP in kidneys.

Enzymatic microelectrode biosensors have many advantages over existing means of measuring analytes *in vivo*. However, special precautions should be used for this approach as for any other new method. Validation with an established approach provides confidence in the obtained data. For instance, microdialysis measurements were made as described previously[26,27]. No significant difference was observed between the peak concentrations determined by the sensors and those obtained from the dialysis samples[12]. The limitation of microdialysis is that it only measures steady-state levels of analyte. As such, the assessment of dynamic changes in cell signaling can only be achieved with the use of the enzymatic microelectrode biosensors. The manufactory specifications of the sensor response times differ between sensor types. *Ex vivo* sensors have a response time of 5-10 sec and *in vivo* sensors of 30-35 sec for the signal rise from 10 to 90%. The calibration traces (**Figures 6** and **7**)

demonstrate the time resolution of analyte addition/removal. For both the sensor and microdialysis approaches, the use of specific enzymes to block the signal produced by analytes is required to ensure specificity.

The described protocols have several challenges. As with any sensor insertion into tissue, tissue damage does occur. This could activate signaling pathways which may influence the measurements[28]. To minimize the cell damage, thinner sensors would be needed. However, it is difficult to penetrate the kidney capsule with the sensors so needles are used to make a small entry hole. Thin sensors are more likely to bend and disrupt their coating on insertion. Larger diameter sensors are more resistant bending and the resultant damage to their coating. **Figure 3** shows a thin and thick sensor. In addition to the thick sensor's resistance to bending, they contain a thicker layer of coating, providing increased protection for the enzymatic layer. The concern of tissue damage caused by using thick sensors was considerably less in kidneys than it would be in brain tissue. The insertion depth is approximated and final placement should be verified after measurements on the kidney are completed. Estimation between the cortex and medulla layers using the sensor tip length as an insertion guide and is sufficient as the sensor tip is 0.5 mm and the kidney cortex is 2-3 mm thick. Fouling of the sensor also occurs at a greater rate in blood, thus limiting the sensor use in long *in vivo* protocols to one experiment. Recording times of 1 to 1 ½ hr resulted in only a small sensor drift. The main criteria when assessing the reduced sensor performance is the low sensitivity to the analyte during calibration process. Increased electrical noise and instability of the baseline current can also indicate that the sensor tip is damaged. For accurate measurements of ATP, both sensors (ATP and Null) should have similar noise and stability characteristics for further subtraction of the signal. Otherwise, one of the sensors should be replaced. For low noise and detection of small concentrations of analyte, the use of new sensors for each animal is suggested.

Several steps are crucial for successful experimental outcomes. The sensors are very fragile and should be handled carefully to avoid damaging the sensor tip. Also, after rehydration, the sensors should not be exposed to the air for more than 20 sec. Low noise recordings are required for the successful detection of biological signals in tissues. For that purpose, a high-performance lab air table and proper electrical grounding is required. The addition of exact amounts of analyte during the calibration steps is necessary for accurate concentration determination in experiments. Achieving good clearing of the kidney in *ex vivo* kidney surgeries will result in successful recordings. The use of enzymes apyrase and catalase in calibrations and in experiments allows for the assessment of sensor nonspecific sensitivity and confirms the measurements.

These protocols provide greatly enhanced detail of extracellular signaling in kidneys. The improved sensitivity and temporal resolution afforded by the sensors may allow us to resolve changes in ATP signaling in disease states and following pharmacological manipulation that were previously undetectable. The *in vivo* protocol is well suited for complex physiological studies while *ex vivo* is optimal for the study of pharmacological applications on kidneys. The design of the *in vivo* sensor used here enables unprecedented resistance against interference in blood-perfused tissue. Taken together, these sensors offer a large amount of applications that were previously not possible with existing protocols and techniques.

Disclosures

Sensors for the video recording of this manuscript were provided by Sarissa Biomedical Limited (Coventry, UK).

Acknowledgements

We appreciate Sarissa Biomedical for their work in developing the sensors used in the present manuscript. This research was supported by the National Heart, Lung, and Blood Institute grants HL108880 (A. Staruschenko), HL 116264 (A. Cowley) and HL 122662 (A. Staruschenko and A. Cowley), a project funded by the Medical College of Wisconsin Research Affairs Committee #9306830 (O. Palygin) and Advancing a Healthier Wisconsin Research and Education Program #9520217, and the Young Investigator Grant of the National Kidney Foundation (O. Palygin).

References

1. Palygin, O., & Staruschenko, A. Detection of endogenous substances with enzymatic microelectrode biosensors in the kidney. *Am J Physiol Regul Integr Comp Physiol.* **305**, R89-91, doi:10.1152/ajpregu.00135.2013 (2013).
2. Clark, L. C., Jr., & Lyons, C. Electrode systems for continuous monitoring in cardiovascular surgery. *Ann N Y Acad Sci.* **102**, 29-45, doi:10.1111/j.1749-6632.1962.tb13623.x (1962).
3. Haruyama, T. Micro- and nanobiotechnology for biosensing cellular responses. *Adv Drug Deliv Rev.* **55**, 393-401, doi:10.1016/S0169-409X(02)00224-7 (2003).
4. Huckstepp, R. T. *et al*. Connexin hemichannel-mediated CO2-dependent release of ATP in the medulla oblongata contributes to central respiratory chemosensitivity. *J Physiol.* **588**, 3901-3920, doi:10.1113/jphysiol.2010.192088 (2010).
5. Lopatar, J., Dale, N., & Frenguelli, B. G. Minor contribution of ATP P2 receptors to electrically-evoked electrographic seizure activity in hippocampal slices: Evidence from purine biosensors and P2 receptor agonists and antagonists. *Neuropharmacology.* **61**, 25-34, doi:10.1016/j.neuropharm.2011.02.011 (2011).
6. Avshalumov, M. V., Chen, B. T., Marshall, S. P., Pena, D. M., & Rice, M. E. Glutamate-dependent inhibition of dopamine release in striatum is mediated by a new diffusible messenger, H2O2. *J Neurosci.* **23**, 2744-2750 (2003).
7. Frenguelli, B. G., Wigmore, G., Llaudet, E., & Dale, N. Temporal and mechanistic dissociation of ATP and adenosine release during ischaemia in the mammalian hippocampus. *J. Neurochem.* **101**, 1400-1413, doi:10.1111/j.1471-4159.2007.04425.x (2007).
8. Lalo, U. *et al*. Exocytosis of ATP from astrocytes modulates phasic and tonic inhibition in the neocortex. *PLoS Biol.* **12**, e1001747, doi:10.1371/journal.pbio.1001747 (2014).
9. Heinrich, A., Ando, R. D., Turi, G., Rozsa, B., & Sperlagh, B. K+ depolarization evokes ATP, adenosine and glutamate release from glia in rat hippocampus: a microelectrode biosensor study. *Br.J Pharmacol.* **167**, 1003-1020, doi:10.1111/j.1476-5381.2012.01932.x (2012).
10. Dale, N. Purinergic signaling in hypothalamic tanycytes: potential roles in chemosensing. *Semin Cell Dev Biol.* **22**, 237-244, doi:10.1016/j.semcdb.2011.02.024 (2011).

11. Gourine, A. V., Llaudet, E., Dale, N., & Spyer, K. M. Release of ATP in the ventral medulla during hypoxia in rats: role in hypoxic ventilatory response. *J Neurosci*. **25**, 1211-1218 (2005).
12. Palygin, O. *et al*. Real-time electrochemical detection of ATP and H2O2 release in freshly isolated kidneys. *Am J Physiol Renal Physiol.*, doi:10.1152/ajprenal.00129.2013 (2013).
13. Thome-Duret, V., Gangnerau, M. N., Zhang, Y., Wilson, G. S., & Reach, G. Modification of the sensitivity of glucose sensor implanted into subcutaneous tissue. *Diabetes Metab*. **22**, 174-178 (1996).
14. Wilson, G. S., & Gifford, R. Biosensors for real-time *in vivo* measurements. *Biosens. Bioelectron*. **20**, 2388-2403, doi:10.1016/j.bios.2004.12.003 (2005).
15. Ilatovskaya, D., & Staruschenko, A. Single-Channel Analysis of TRPC Channels in the Podocytes of Freshly Isolated Glomeruli. *Methods Mol Biol*. **998**, 355-369, doi:10.1007/978-1-62703-351-0_28 (2013).
16. Stockand, J. D., Vallon, V., & Ortiz, P. *In vivo* and *ex vivo* analysis of tubule function. *Compr Physiol.* **2**, 2495-2525, doi:10.1002/cphy.c100051 (2012).
17. Turner, A. P. Biosensors: Fundamentals and applications - Historic book now open access. *Biosens. Bioelectron*. **65C**, A1, doi:10.1016/j.bios.2014.10.027 (2014).
18. Kauffmann, J. M., & Guilbault, G. G. Enzyme electrode biosensors: theory and applications. *Methods Biochem Anal.* **36**, 63-113, doi:10.1002/9780470110577.ch3 (1992).
19. Barlett, P. N., & Cooper, J. M. A review of the immobilization of enzymes in electropolymerized films. *J Electroanal Chem.* **362**, 1-12, doi:10.1016/0022-0728(93)80001-X (1993).
20. Kano, K., Morikage, K., Uno, B., Esaka, Y., & Goto, M. Enzyme microelectrodes for choline and acetylcholine and their applications. *Anal Chim Acta.* **299**, 69-74, doi:10.1016/0003-2670(94)00318-1 (1994).
21. Llaudet, E., Hatz, S., Droniou, M., & Dale, N. Microelectrode biosensor for real-time measurement of ATP in biological tissue. *Anal Chem.* **77**, 3267-3273 (2005).
22. Llaudet, E., Botting, N. P., Crayston, J. A., & Dale, N. A three-enzyme microelectrode sensor for detecting purine release from central nervous system. *Biosens Bioelectron.* **18**, 43-52, doi:10.1016/S0956-5663(02)00106-9 (2003).
23. Cosnier, S., Lepellec, A., Guidetti, B., & Isabelle, R.-L. Enhancement of biosensor sensitivity in aqueous and organic solvents using a combination of poly(pyrrole-ammonium) and poly(pyrrole-lactobionamide) films as host matrices. *J Electroanal Chem.* **449**, 165-171, doi:10.1016/S0022-0728(98)00049-7 (1998).
24. Gourine, A. V. *et al*. Astrocytes control breathing through pH-dependent release of ATP. *Science.* **329**, 571-575 (2010).
25. Kluess, H. A., Stone, A. J., & Evanson, K. W. ATP overflow in skeletal muscle 1A arterioles. *J. Physiol*. **588**, 3089-3100, doi:10.1113/jphysiol.2010.193094 (2010).
26. Nishiyama, A., Jackson, K. E., Majid, D. S., Rahman, M., & Navar, L. G. Renal interstitial fluid ATP responses to arterial pressure and tubuloglomerular feedback activation during calcium channel blockade. *Am J Physiol Heart Circ Physiol.* **290**, H772-777, doi:10.1152/ajpheart.00242.2005 (2006).
27. Jin, C. *et al*. Effects of renal perfusion pressure on renal medullary hydrogen peroxide and nitric oxide production. *Hypertension.* **53**, 1048-1053 (2009).
28. Khan, A. S., & Michael, A. C. Invasive consequences of using micro-electrodes and microdialysis probes in the brain. *Trends Anal. Chem.* **22**, 503-508, doi:10.1016/S0165-9936(03)00908-7 (2003).

